A nonlinear boundary-value problem with an integral constraint

Dedicated to Professor Yasumasa Nishiura on the occasion of his 60th birthday

By

Hisashi OKAMOTO*

Abstract

We consider a boundary-value problem $u'' + Ru^2 = f(R, x)$, where f is a given function, and $u'' + Ru^2 = \text{constant} + f(R, x), \int_{-\pi}^{\pi} u(x)\,\mathrm{d}x = 0$. We demonstrate that the integral constraint yields a considerable difference in the structure of bifurcation. If $\int_{-\pi}^{\pi} u(x)\,\mathrm{d}x = 0$ is present, a strange bifurcation diagram exists.

§1. Introduction

We consider simple nonlinear boundary-value problems with a prescribed source term and study the dependence of the solutions on the source term. Specifically, we consider the following two equations. The first one is:

$$(1.1) \qquad u'' + Ru^2 + f(R, x) = 0 \qquad (-\pi < x < \pi),$$

where $R > 0$ is a parameter and the prime implies differentiation. $u = u(x)$ $(-\pi < x < \pi)$ is an unknown function and $f = f(R, x)$ is a given function. Throughout this paper, we consider equations with the periodic boundary condition. The second one is the following coupled system:

$$(1.2) \qquad u'' + Ru^2 + f(R, x) - \frac{1}{2\pi} \int_{-\pi}^{\pi} \left(Ru(x)^2 + f(R, x) \right)\,\mathrm{d}x = 0,$$

$$(1.3) \qquad \int_{-\pi}^{\pi} u(x)\,\mathrm{d}x = 0.$$

Namely this is the nonlinear equation (1.1) with the integral constraint (1.3). The nonlinear term u^2 can be a more general one, but, since the simple choice u^2 is already interesting enough, we restrict ourselves to the case of u^2 in the present paper.

Let us use the usual $L^2(-\pi, \pi)$ as the function space where we search solutions. Then the only difference between (1.1) and (1.2)(1.3) is whether we consider the differential equation in $L^2(-\pi, \pi)$ or in $\dot{L}^2(-\pi, \pi)$, where

$$\dot{L}^2(-\pi, \pi) = \left\{ g \in L^2(-\pi, \pi) \;\middle|\; \int_{-\pi}^{\pi} g(x)\,\mathrm{d}x = 0 \right\}.$$

Let P denotes the orthogonal projection from L^2 onto $\dot{L}^2$. Then the system (1.2)(1.3) is expressed as

$$u'' + RP(u^2) + Pf = 0 \qquad (u \in \dot{L}^2).$$

It seems to us that (1.1) has been studied well and only a little may be left for serious study. However, (1.2)(1.3) may not be so. In fact we will show that the equation (1.1) and the coupled system (1.2)(1.3) have considerable differences, which seem to have been unnoticed so far. In what follows we explain why the constrained equation is interesting, how much different it is from (1.1), and whatever consequences it produces.

§ 2.   Background

We now explain why we are interested in these equations. Let us consider time-dependent versions without an external source f:

(2.1) $$u_t = u_{xx} + u^2;$$

(2.2) $$u_t = u_{xx} + u^2 - \frac{1}{2\pi} \int_{-\pi}^{\pi} u(t, x)^2 \,\mathrm{d}x,$$

where the subscript implies the differentiation. With the periodic boundary condition, they are considered to be an evolution equation in $L^2(-\pi, \pi)$ and $\dot{L}^2(-\pi, \pi)$, respectively. It is known that if $u(0, x) \geq 0$ and is not identically zero, then the solution of (2.1) with the periodic boundary condition blows up in finite time. Namely there exists a finite T such that

$$\lim_{t \uparrow T} \int_{-\pi}^{\pi} u(t, x)\,\mathrm{d}x = +\infty.$$

For (2.2), a solution exists globally in time if its initial data is small. On the other hand, some solutions blow up in finite time if their initial data are large. The proof of the last proposition is more complicated than (2.1): Existence of blow-ups in (2.2) was proved by [1]. Later a simpler proof was discovered by [9]. As t approaches the blow-up time, the solution of (2.1) remain bounded at all but finite point x. See [2, 10]. The

situation is very different for (2.2), where "blow-up everywhere" occurs in the sense that $|u(t, x)| \to \infty$ for all x as $t \uparrow T$. However, u is dominantly large at a certain point in the sense that $u(t, x_0) \to +\infty$ at some x_0, and at the same time, $\lim_{t \to T} u(t, x)/u(t, x_0) = 0$ if $x \neq x_0$. As far as we know, the blow-up problem (2.2) is far from being well-studied. See [9].

(2.2) arises if we approximate self-similar solutions of the two-dimensional Navier-Stokes equations; [1, 9]. Stationary solutions of (2.2) arise in Oseen's stationary flow of incompressible viscous fluid; [3, 4, 8].

There is another reason why the author is interested in the equation with integral constraint. It is rather tempting to believe that a simple input produces only a simple output. For instance,

$$-u'' + a^2 u = \cos nx$$

has a solution $u = \frac{1}{n^2 + a^2} \cos nx$, which has as many peaks as the input $\cos nx$. But the author found an interesting phenomena: in some equations the bifurcating solutions exist and tend to a very simple function as $R \uparrow \infty$. For instance, if we consider the Proudman-Johnson equation, even if the driving force is $\sin nx$ or $\cos nx$ with $n = 2, 3, \cdots, 10$, the solution tends to a constant times $\sin x$. Namely the simplest solution appears despite the complexity of the driving force, see [6, 7]. This phenomenon is universal in the sense that for any n the solution tends to a constant multiple of $\sin x$ if R tends to infinity. This phenomenon does not occur in a simple reaction-diffusion equation, see [5]. Accordingly, the author wonders for what equation such a universal unimodal solution exists. And he was led to an equation somewhere between the 2D Navier-Stokes equations and the reaction-diffusion equation. That is the one we are going to consider in the present paper. With these observations, the author wishes to compute more examples in the present paper.

§3.   Bifurcation

We now consider the following boundary-value problem:

$$(3.1) \qquad u'' + Ru^2 - \frac{R}{2} + \ell^2 \cos \ell x - \frac{R}{2} \cos 2\ell x = 0 \qquad (-\pi < x < \pi),$$

where ℓ is a non-negative integer. The external source $f(R, x)$ has been chosen so that $u = \cos \ell x$ becomes a solution for all $R > 0$. We consider only those solutions which is even in x. We may therefore equivalently rewrite the equation as

$$(3.2) \quad u'' + Ru^2 - \frac{R}{2} + \ell^2 \cos \ell x - \frac{R}{2} \cos 2\ell x = 0 \qquad (0 < x < \pi), \quad u'(0) = u'(\pi) = 0.$$

Numerical computations are performed by the spectral method. We thus set

$$u^N = \sum_{n=0}^{N} a_n \cos nx.$$

With $N = 100$ most solutions were easily computed. However, if R is very large, we needed a larger N. For instance, we took $N = 1000$ if $R = 10000$.
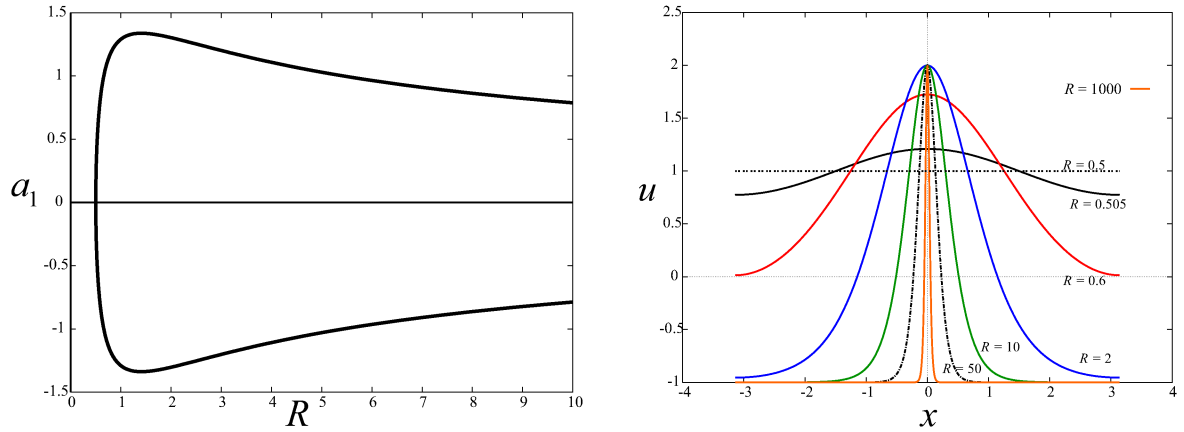

Figure 1. $\ell = 0$. (left) Bifurcation diagram, where the Fourier coefficient a_1 is plotted against R. A pitchfork bifurcates at $R = 1/2$. (right) Profiles of the bifurcating solutions: $\ell = 0, R = 0.505, 0.6, 2, 10, 50$, and $R = 1000$.

§3.1. $\ell = 0$

If $\ell = 0$, the equation is well-known. In fact, we have $u_{xx} + R(u^2 - 1) = 0$ in $0 < x < \pi$ with the Neumann boundary conditions at $x = 0, \pi$. The solutions can be represented by the elliptic functions. Note that if $u(x)$ is a solution for $R = R'$ and if m is a positive integer, then $u(mx)$ is a solution for $R = m^2 R'$. We therefore compute only those solutions which take their maximum at $x = 0$ and are monotone decreasing in $0 < x < \pi$. We call such a solution a solution of mode one. The solution $(m^2 R, u(mx))$ is called a solution of mode m. Since the linearized operator $v'' + 2Rv = 0$ has an eigenfunction $v = \cos x$ at $R = 1/2$, the branch of solutions of mode one bifurcates at $R = 1/2$. The diagram is shown in Figure 1 (left). Profiles of the solutions are drawn in Figure 1 (right). They show that

$$\lim_{R \to \infty} u(0) = 2, \qquad \lim_{R \to \infty} u(x) = -1 \quad (x \neq 0).$$

This can be proved rigorously if we represent the solution by elliptic functions. We omit the proof, however.

Along those solutions we computed eigenvalues of the linearized operator to find that no secondary bifurcation occurs in $1/2 < R < 1000$. We also computed eigenvalues for solutions of mode two to find that secondary bifurcation does not occur in $2 < R < 1000$.

§ 3.2. $\ell = 1$

We now consider (3.1) with $\ell = 1$. There exist many bifurcation points along the trivial solution $\cos x$. They appear at approximately $R = 5.32, 17.35, 36.26, 62.04$ etc., which we verified by computing the eigenvalue problem of the linearized operator by $N = 300$. The first three bifurcations are drawn in Figure 2. Here all the bifurcations are transcritical. Bifurcating solutions from the primary bifurcation point, $R \approx 5.32$, are shown in Figures 3 and 4. As we trace these solutions up to $R = 1000$, the solutions show a peculiar interior layers. See Figure 5.
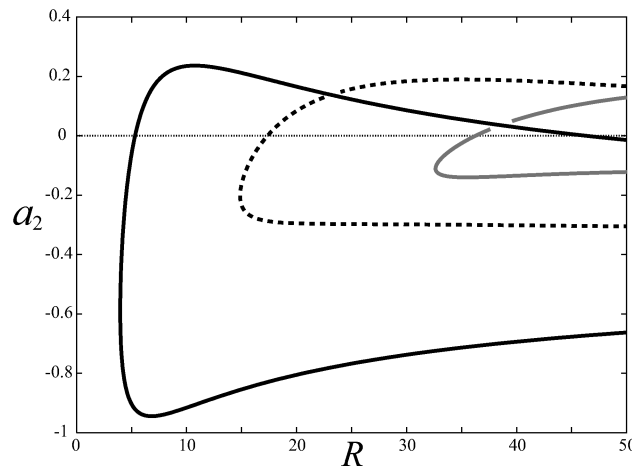
Figure 2. Bifurcation diagram. $\ell = 1$.

Apart from these solutions, there exist many solutions which do not arise from the bifurcation from the trivial solution. If we add these solution branches, the bifurcation diagram looks like Figure 6. Solutions of $R = 1000$ are shown in Figures 7, 8, 9, and 10

§ 3.3. $\ell = 2$

The case where $\ell = 2$ was considered in [6, 7]. Non-trivial solutions branch off the trivial solution at $R \approx 0.908$. They form a supercritical pitchfork as is shown in Figure 11 (left). The nontrivial solutions extend indefinitely to $R \to \infty$. If we look at the solutions at very large R we did not find any unimodality: u'' has three crests and three troughs, see [6].

As far as we computed up to $R = 10000$, there was no other bifurcation point on the branch of the trivial solution, and we concluded that $R = 0.908 \cdots$ was the only bifurcation point at the trivial solution.

These were obtained in [6]. There was no other bifurcation from the trivial solution, but we did not examine secondary bifurcation from the non-trivial solutions. We exam-
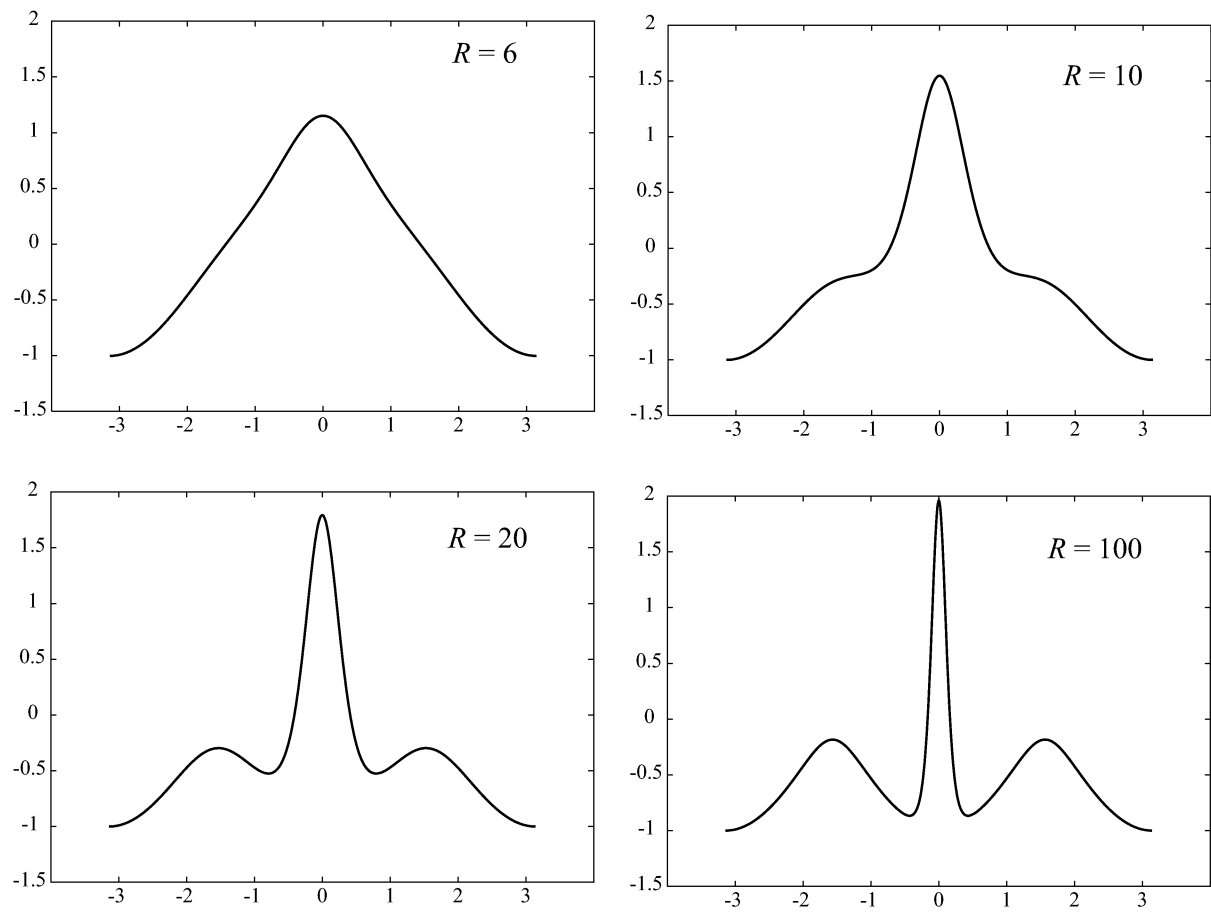
Figure 3. Graphs of solutions from $R = 6$ to $R = 100$. The upper part of the leftmost bifurcating branch in Figure 2. $\ell = 1$.
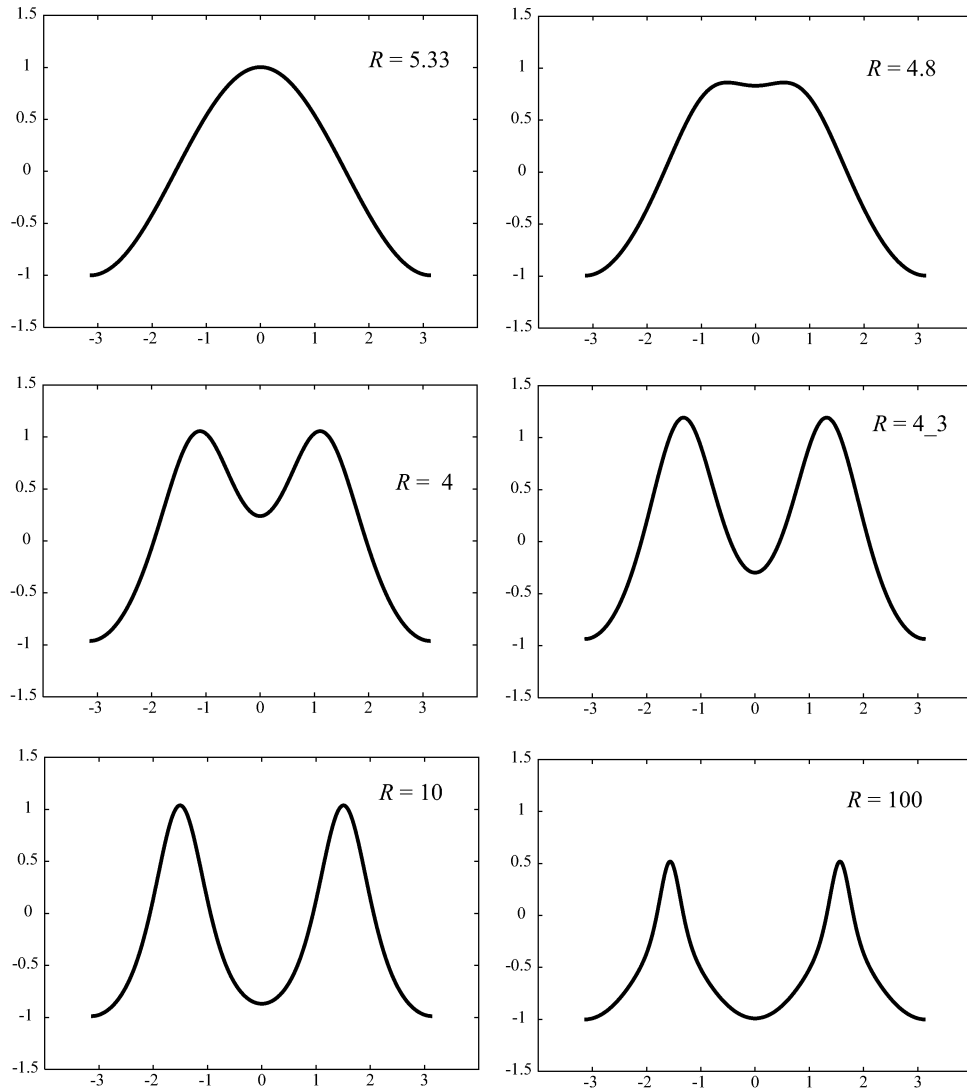
Figure 4. Graphs of solutions on the lower part of the leftmost bifurcating branch in Figure 2. $\ell = 1$.
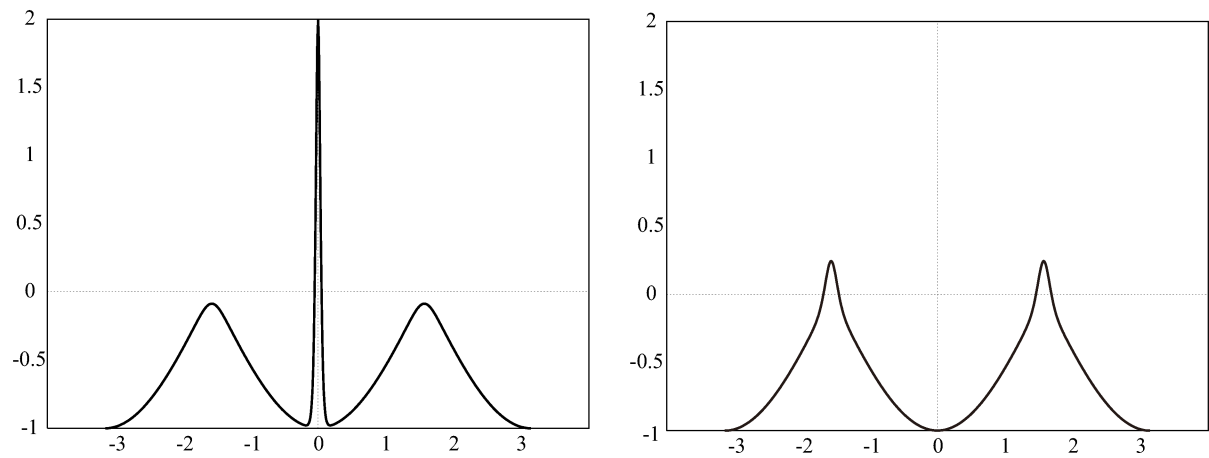
Figure 5. Two solutions at $R = 1000$, bifurcating from the primary bifurcation point. $\ell = 1$.
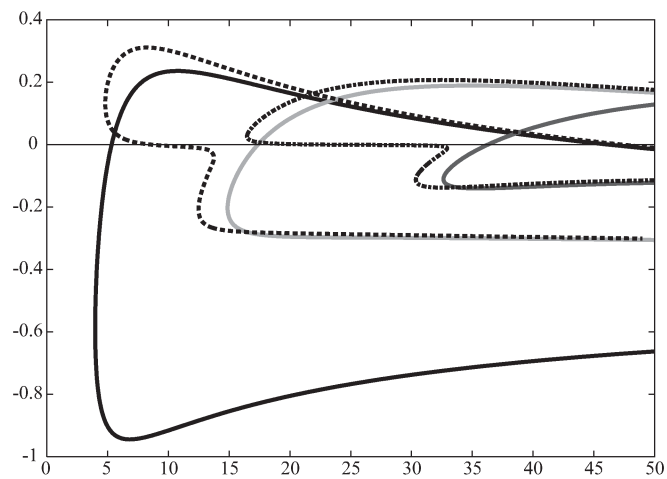

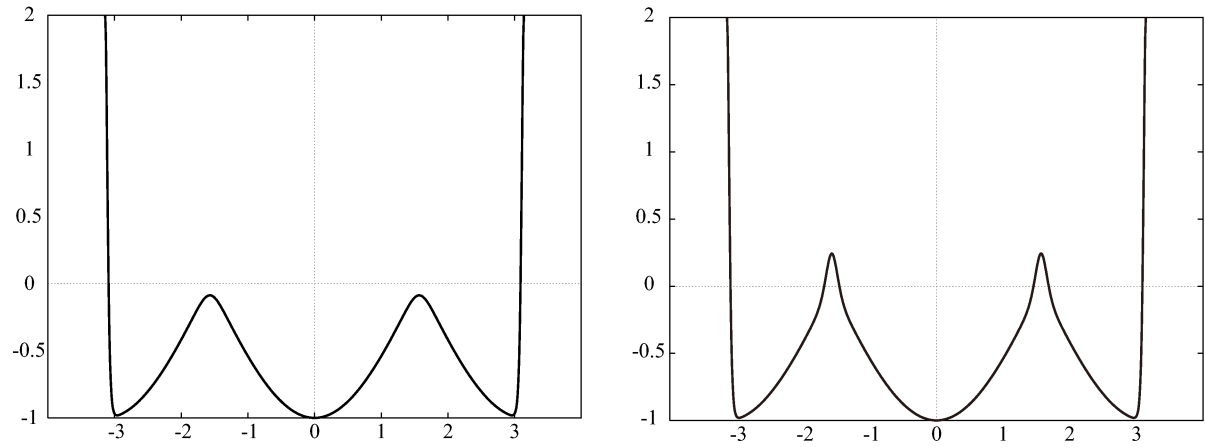Figure 6. Bifurcation diagram. $\ell = 1$. Solid lines represent branches which bifurcate from the trivial solutions. Broken lines represent those branches which are separated from the trivial solutions.
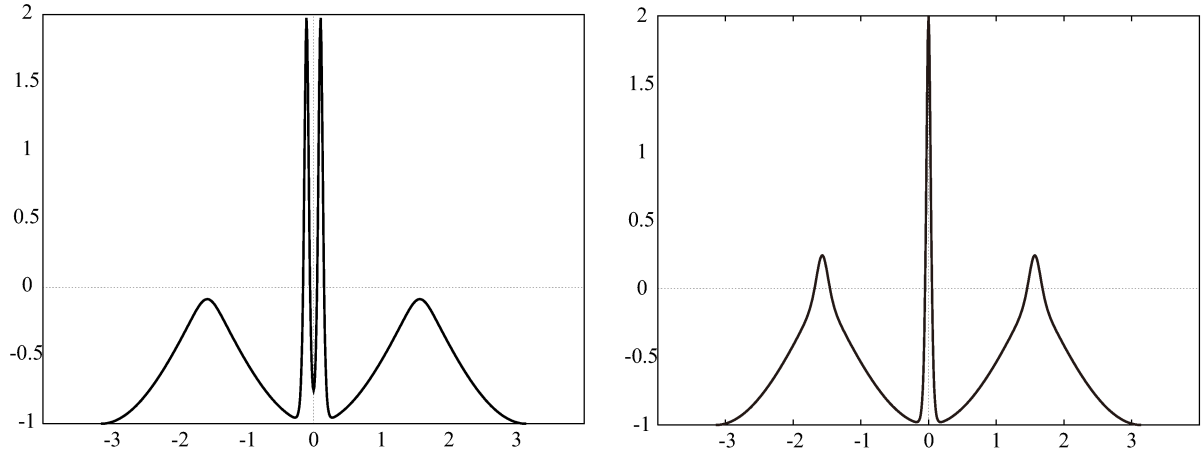
Figure 7. Two solutions at $R = 1000$, bifurcating from the second bifurcation point. $\ell = 1$.
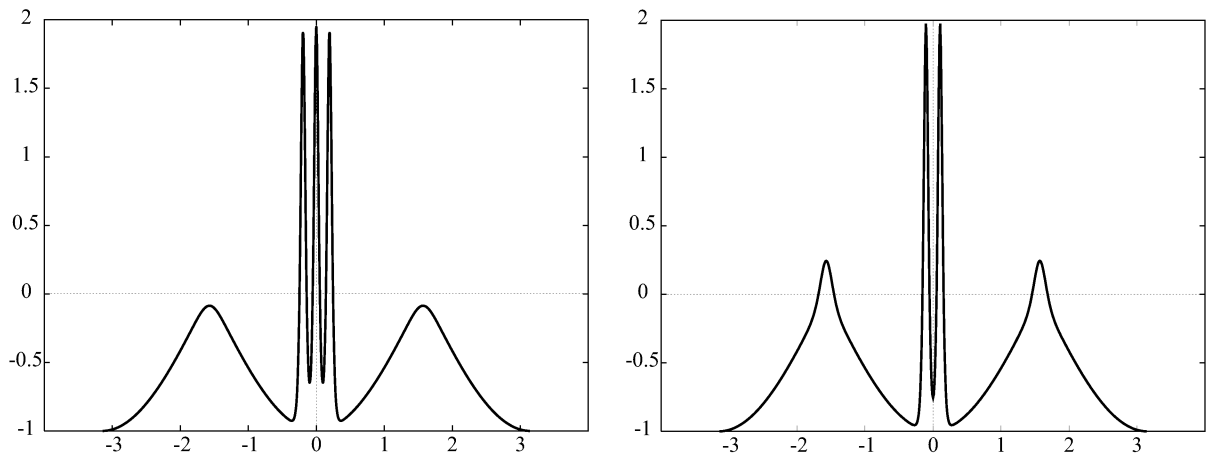
Figure 8. Two solutions at $R = 1000$, bifurcating from the third bifurcation point. $\ell = 1$.

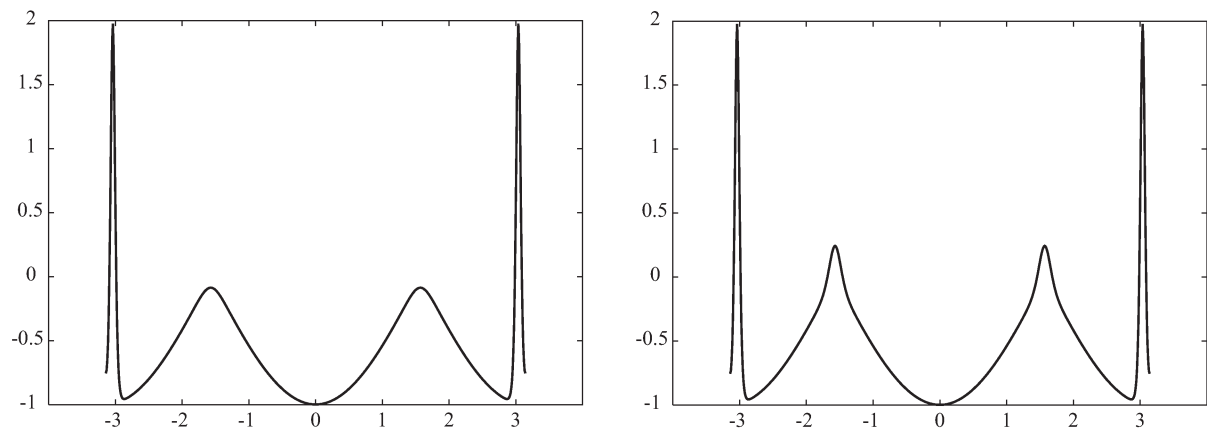Figure 9. Two solutions at $R = 1000$, on the branch separated from the trivial solutions. $\ell = 1$.

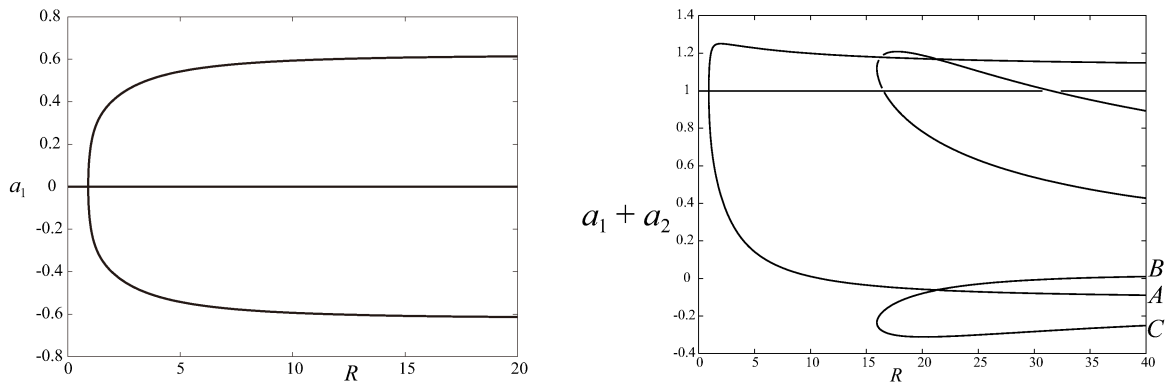Figure 10. Two solutions at $R = 1000$, on the branch separated from the trivial solutions. $\ell = 1$.

Figure 11. (left) Bifurcation diagram of (3.1) in (R, a_1). $\ell = 2$. This diagram is taken from [6]. (right) the diagram in $(R, a_1 + a_2)$. Secondary branches are added.

ined this in the present paper and found secondary branches bifurcating at $R \approx 21.3$. The bifurcation is transcritical. The diagram is shown in Figure 11 (right).

At $R = 40$ we have six non-trivial solutions, three of which are depicted in Figure 12 (left). Other solutions are obtained by the shift $u(x) \mapsto u(x + \pi)$. Solutions on the secondary branch exhibit a sharp spine at $R = 10000$, see Figure 12 (right). It is interesting that three solutions agree well with one another in $\pi/2 \le |x| \le \pi$ if $R = 40$. If $R = 10000$, they differ significantly only in $-1 \le x \le 1$. We however do not know why this happens.

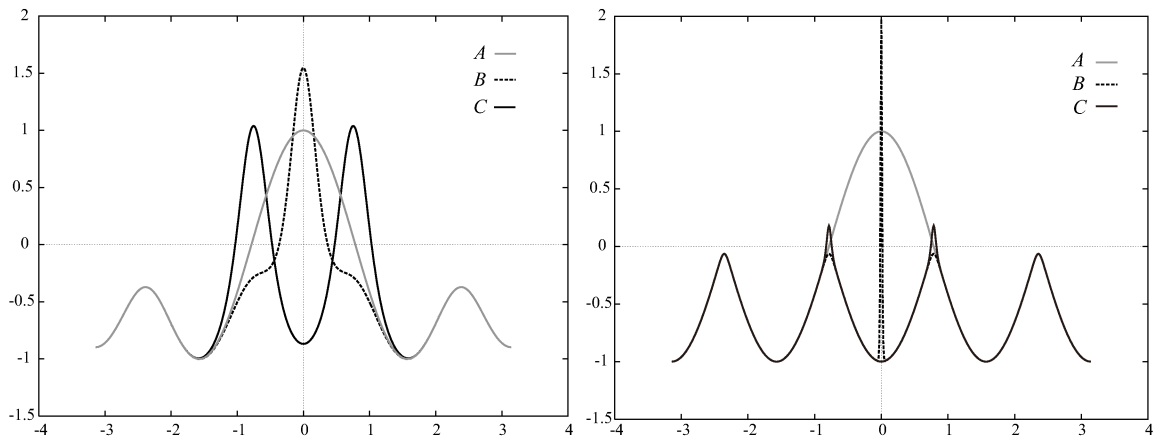Figure 12. (left) Graphs of the bifurcating solutions u of (3.1) at $R = 40$. (right) Graphs at $R = 10000$. $A, B,$ and C correspond to those marked in Figure 11.

$$§ \, \mathbf{3.4.} \qquad \ell = 3$$

If $\ell = 3$, we obtain Figure 13(left) as the diagram. Non-trivial solutions bifurcate at around $R \approx 1.729$. The bifurcation is transcritical.

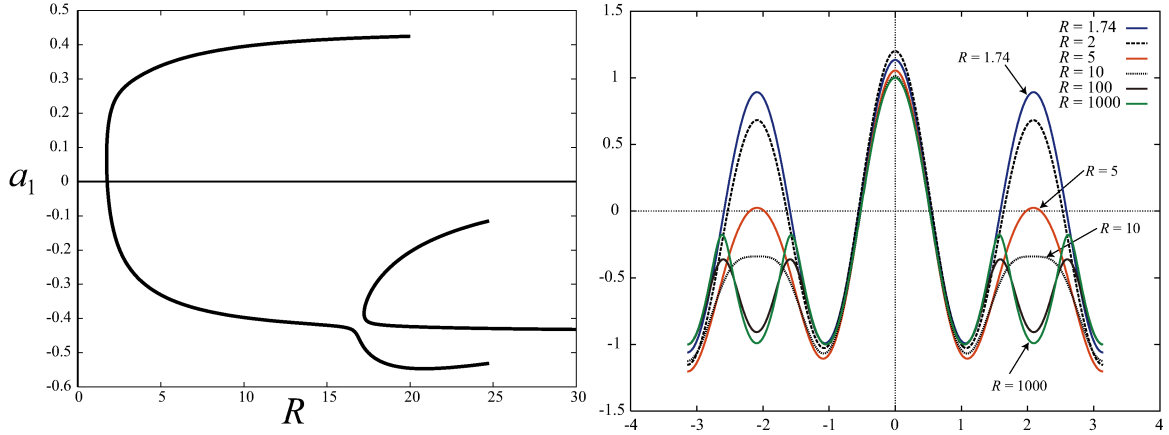There are four non-trivial solutions at $R = 1000$. They are drawn in Figure 14.

Figure 13. (left) Bifurcation diagram of (3.1) in (R, a_1). $\ell = 3$. (right) Graphs of u in the upper part of the branch.

§ 4.   Constrained equation

We now compare (3.1) with the following problem for $\ell \geq 1$:

$$(4.1) \quad u'' + Ru^2 + \ell^2 \cos \ell x - \frac{R}{2} \cos 2\ell x - \frac{R}{2\pi} \int_{-\pi}^{\pi} u(x)^2 \, \mathrm{d}x = 0, \qquad \int_{-\pi}^{\pi} u(x) \, \mathrm{d}x = 0.$$

Again, the external force is chosen so that $u = \cos \ell x$ becomes a solution.

For $\ell = 0$, we consider the following equation:

$$(4.2) \quad u'' + R \left(u^2 - \frac{1}{2\pi} \int_{-\pi}^{\pi} u(x)^2 \, \mathrm{d}x \right) = 0 \quad (-\pi < x < \pi), \qquad \int_{-\pi}^{\pi} u(x) \, \mathrm{d}x = 0.$$

$u \equiv 0$ is a trivial solution. The linearized operator shows that there is no bifurcation from it. Non-trivial solutions exist. In fact, if we consider Oseen's spiral flow of the Navier-Stokes equation, the author found in [8] that the 2D Navier-Stokes equations are reduced to

$$U'' + AU = U^2 - \frac{1}{2\pi} \int_{-\pi}^{\pi} U(x)^2 \, \mathrm{d}x \quad (-\pi < x < \pi), \qquad \int_{-\pi}^{\pi} U(x) \, \mathrm{d}x = 0,$$
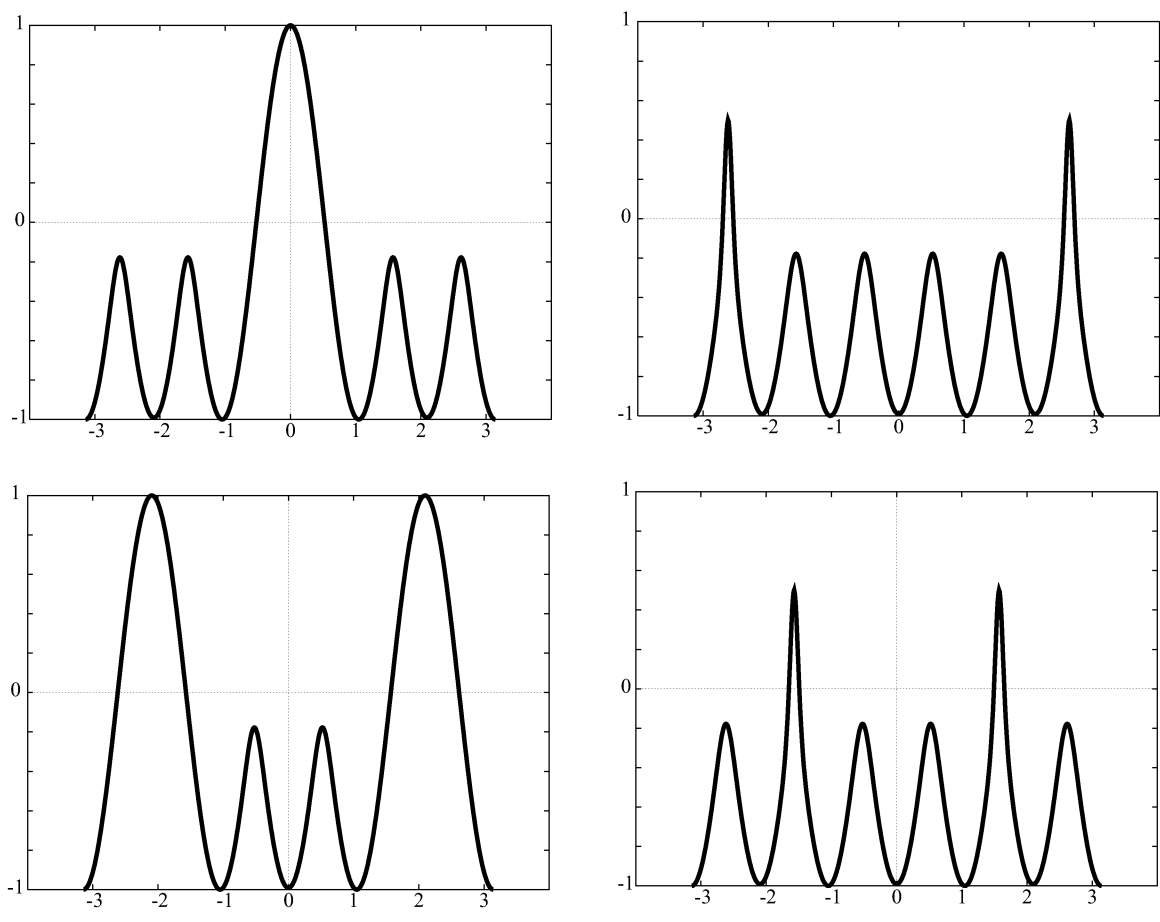
Figure 14. Graphs of u of (3.1) at $R = 1000$. $\ell = 3$.

where A is a real parameter. He showed that a solution exists for all $A \in \mathbb{R}$, in particular, for $A = 0$. Later the properties of the solutions were analyzed by [3, 4]. If U solves

$$(4.3) \qquad U'' = U^2 - \frac{1}{2\pi} \int_{-\pi}^{\pi} U(x)^2 \, \mathrm{d}x \quad (-\pi < x < \pi); \qquad \int_{-\pi}^{\pi} U(x) \, \mathrm{d}x = 0,$$

then $u = -\frac{1}{R}U$ solves (4.2). The graph of U is given in Figure 16 (right). The solution of (4.3) can be represented by the elliptic functions, see [4].

§4.1. $\ell = 1$

Set $\ell = 1$. Then we obtain

$$(4.4) \qquad u'' + Ru^2 + \cos x - \frac{R}{2} \cos 2x - \frac{R}{2\pi} \int_{-\pi}^{\pi} u(x)^2 \, \mathrm{d}x = 0, \qquad \int_{-\pi}^{\pi} u(x) \, \mathrm{d}x = 0.$$

$u = \cos x$ is a solution for all $0 < R < \infty$. A bifurcation occurs transcritically at $R \approx 1.89$, as is shown in Figure 15. Along the branch in $0 < R < 1.89$, the solution becomes bigger in the way that Ru tends to a certain limit as $R \downarrow 0$, see Figure 16. Asymptotic behavior as $R \downarrow 0$ can easily be guessed. Set $u = \frac{1}{R}\phi$ and let R tend to zero. We then obtain

$$(4.5) \qquad \phi'' + \phi^2 - \int_{-\pi}^{\pi} \phi(x)^2 \, \mathrm{d}x = 0, \qquad \int_{-\pi}^{\pi} \phi(x) \, \mathrm{d}x = 0,$$

which is the equation we obtained when $\ell = 0$ ((4.2) with $R = 1$). Its solution matches very well with Ru, as Figure 16 (right) demonstrates.

On the right hand side of the bifurcation point, the bifurcating solutions behave very curiously. They move from the bifurcation point to the right. Then a turning point (limit point) appears at around $R \approx 5.7$. They then move to the left and another turning point appears at around $R \approx 2.79$. Solutions then move to the right and merge the trivial solution at around $R \approx 10$. This bifurcation is again transcritical and the branch moves to the right. This pattern from the trivial solution to the trivial solution at higher R is repeated, as is shown in Figure 15 (c). As a result, the branch constitutes a spiral curve with occasional merges with the trivial solution.

The solution changes from a simple unimodal function (= trivial solution, $u = \cos x$) to a two-peak solution during its course from $R = 1.89$ to $R = 10$. See Figures 17 and 18. It comes back to the trivial solution at $R \approx 10$, but in the right hand side of the second bifurcation point, it shows a three-peak profile. See Figure 19.

We now see that as R increases the number of the peaks of the solution increases or decreases as: $1 \to 2 \to 1 \to 3 \to 1 \to 4$ and so forth. For example, in $115 < R < 125$, the metamorphose of the solutions is shown in Figure 20. They have seven peaks.
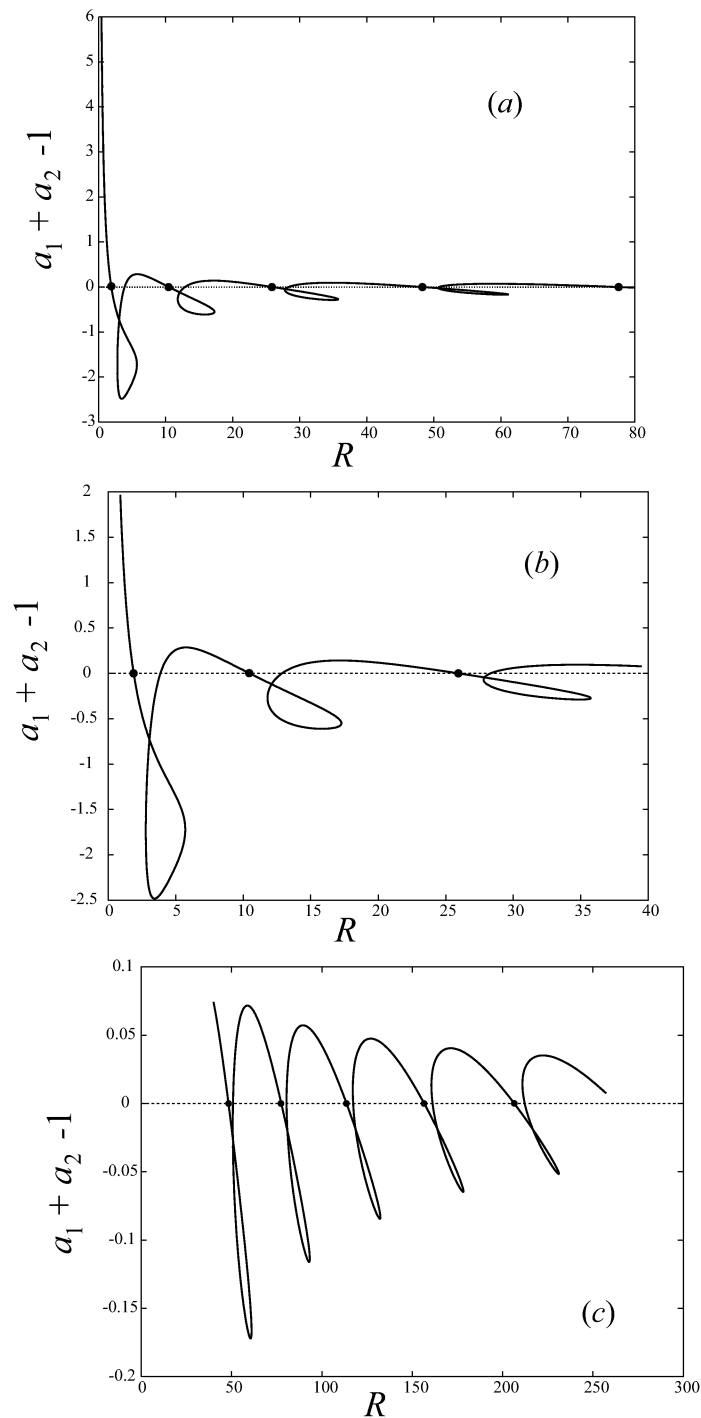
Figure 15. Bifurcation diagrams. $\ell = 1$. (a) $0 < R < 80$. (b) $0 < R < 40$. (c) $40 < R < 250$. Intersections with the horizontal axis marked by a small disk are bifurcation points. Those intersections without a mark are not a bifurcation point: They simply occur because of the projection onto the $(a_1 + a_2 - 1, R)$ plane.
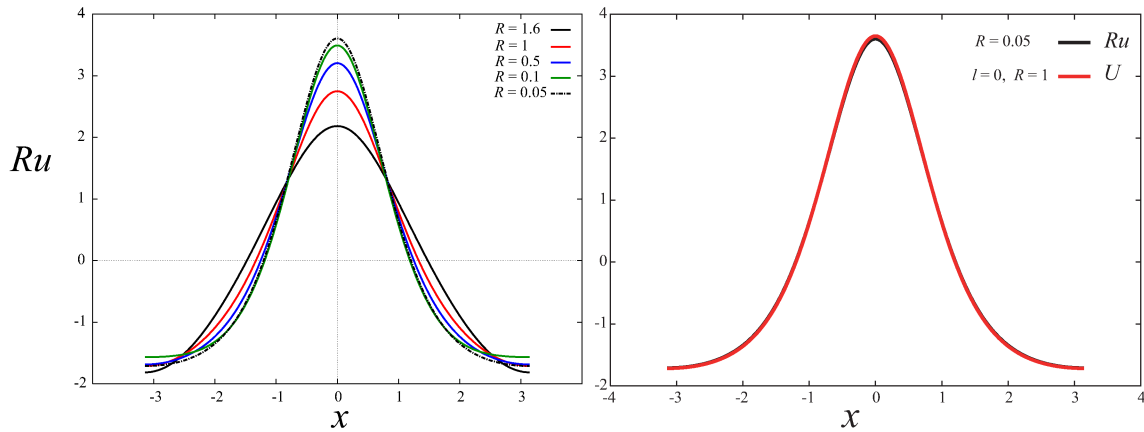
Figure 16. Profiles of bifurcating solutions. $\ell = 1$. Various solutions in $0.005 < R < 1.8$ (left). Solution of (4.3) versus Ru of (4.4).

§4.2. $\ell = 2$

Set $\ell = 2$. Then $u = \cos 2x$ is a solution for all $0 < R < \infty$. A bifurcation occurs at $R = 0.908\cdots$. This critical Reynolds number is almost identical with the one in section 3. But in the present case, it produces a subcritical pitchfork. Along the branch, R decreases monotonically and a_1 increases indefinitely, see Figure 21 (left). Figure 21 (right) clearly shows that as R decreases toward zero, u transforms itself from a two-peaked functions to a single-peaked function. It is not difficult to see that $u(x) \sim R^{-1}\phi(x)$, where ϕ is given by (4.5).

There exists another bifurcation point at $R = 7.58\cdots$, see Figure 22. The branch is transcritical and the left branch extends to the left toward $R \to 0$. The solutions diverge in the sense that $\lim_{R\downarrow 0} Ru$ exists. As Figures 23 and 24 show, these solutions are $(4R, u(2x))$, where (R, u) is the solution of (4.4).

§5.   Concluding remarks

We have found a bifurcation branch where, as R increases, the number of the peaks of the solution increases in such a way that: $1 \to 2 \to 1 \to 3 \to 1 \to 4$ and so forth. A big question is: Does this spiral structure repeat indefinitely? It is likely to do, but we have no way of proving it. Also, we do not have an intuitive explanation for that phenomena.
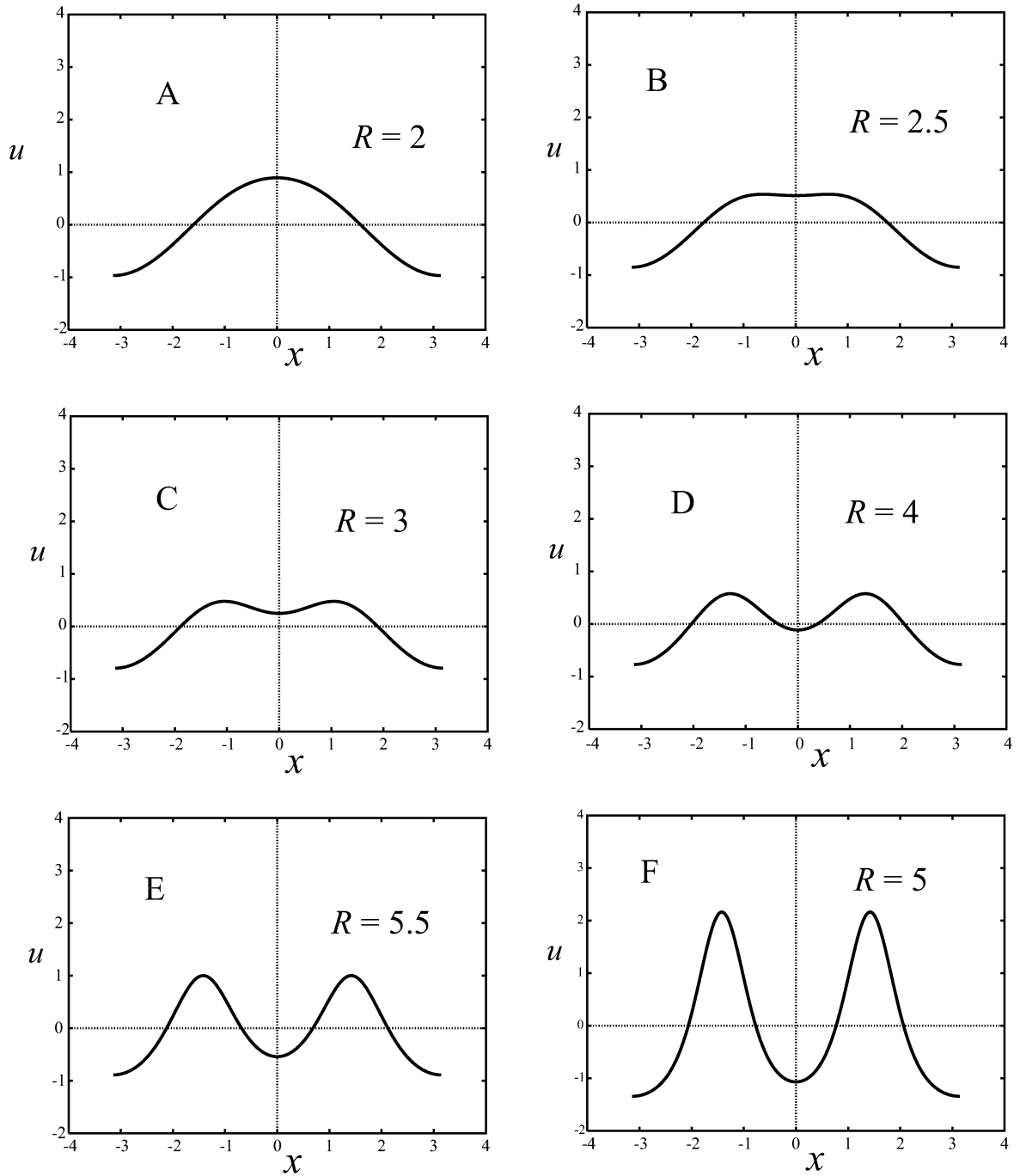
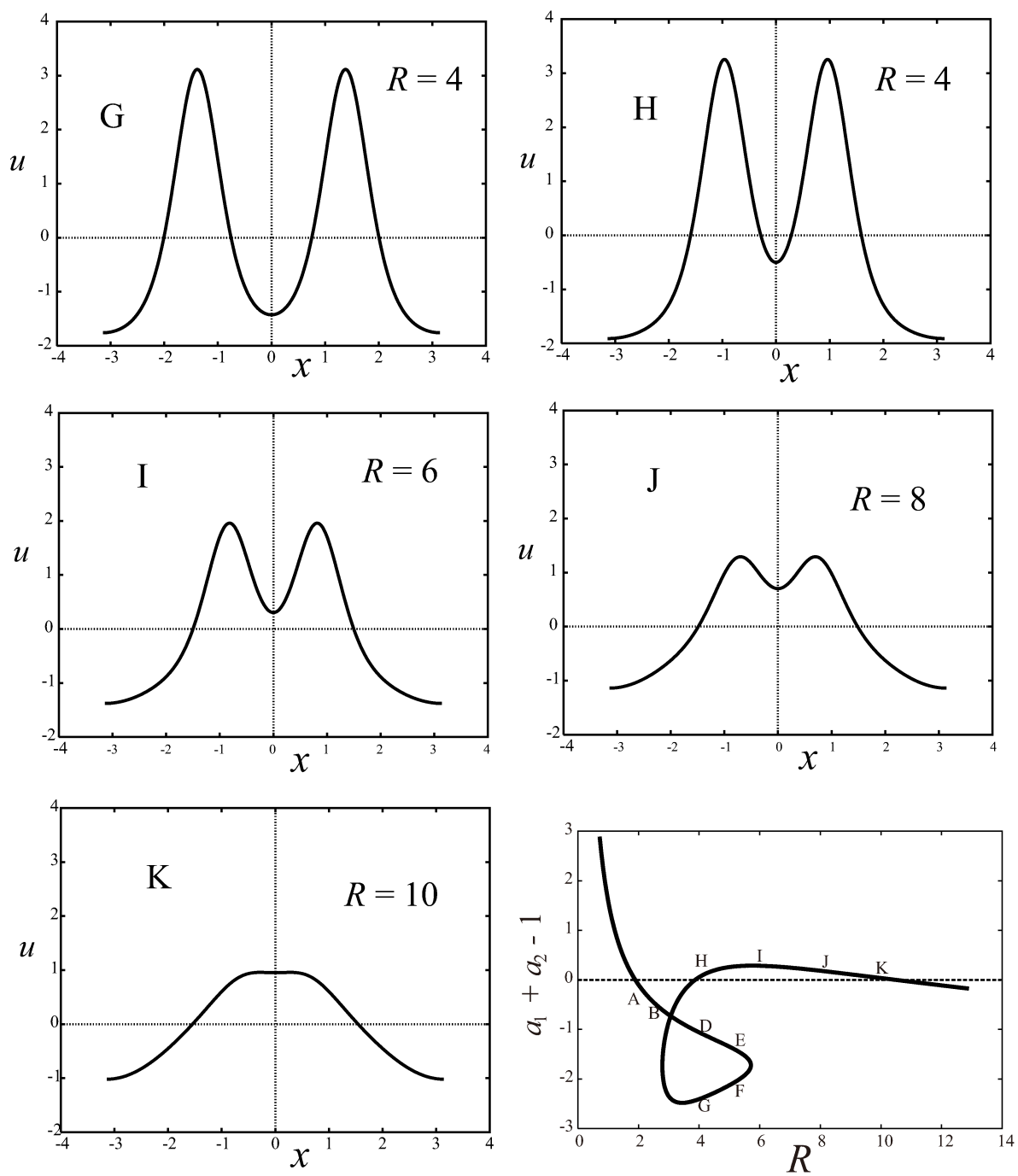Figure 17. Profiles of bifurcating solutions. $\ell = 1$. (a) $2 < R < 10$.

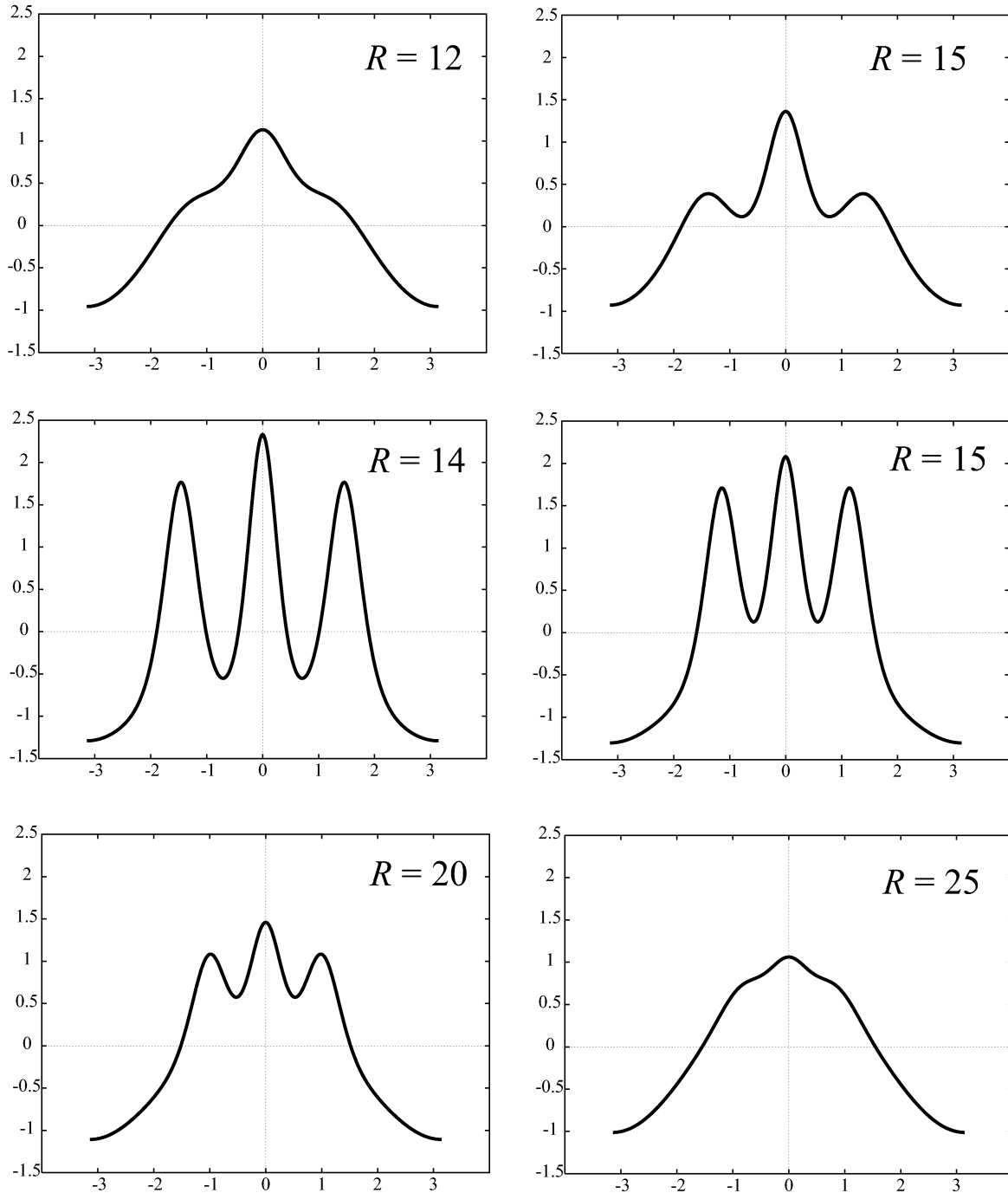Figure 18. Profiles of bifurcating solutions. $\ell = 1$. (a) $2 < R < 10$.

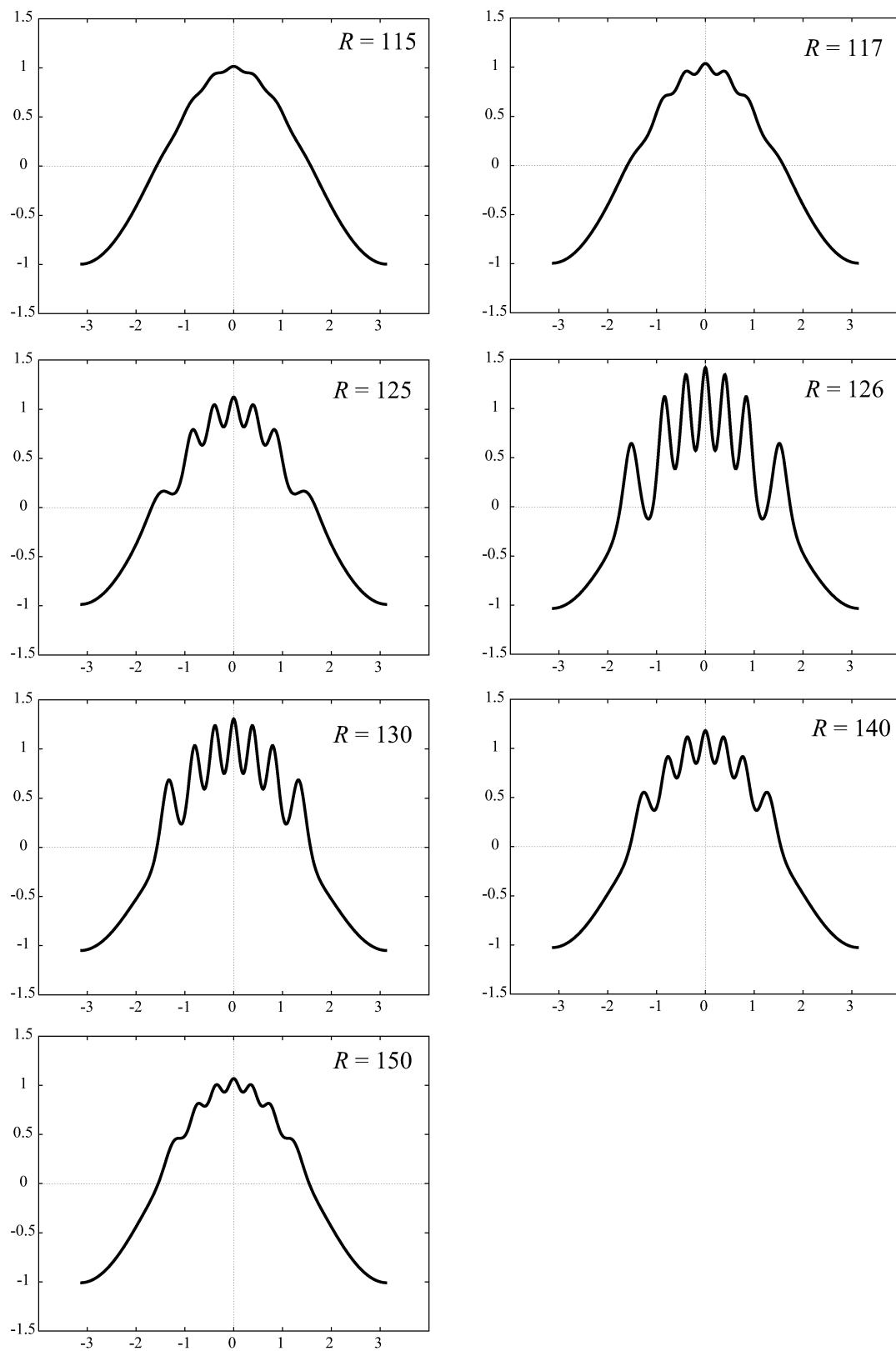Figure 19. Profiles of bifurcating solutions. $\ell = 1$. $12 < R < 25$.

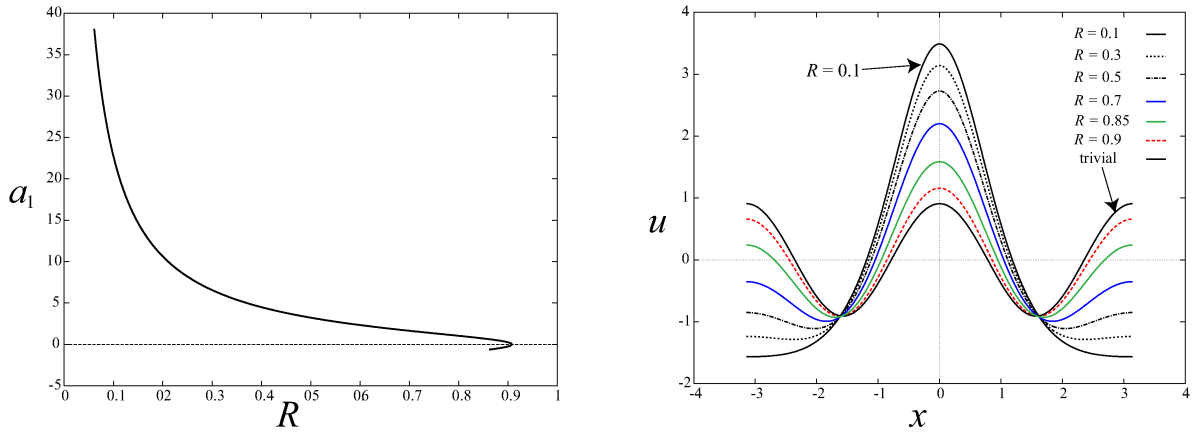Figure 20. Profiles of bifurcating solutions. $\ell = 1$. $115 < R < 160$.

Figure 21. (left): Bifurcation diagrams. (right): Graphs of u for $0.1 \leq R \leq 0.908$.
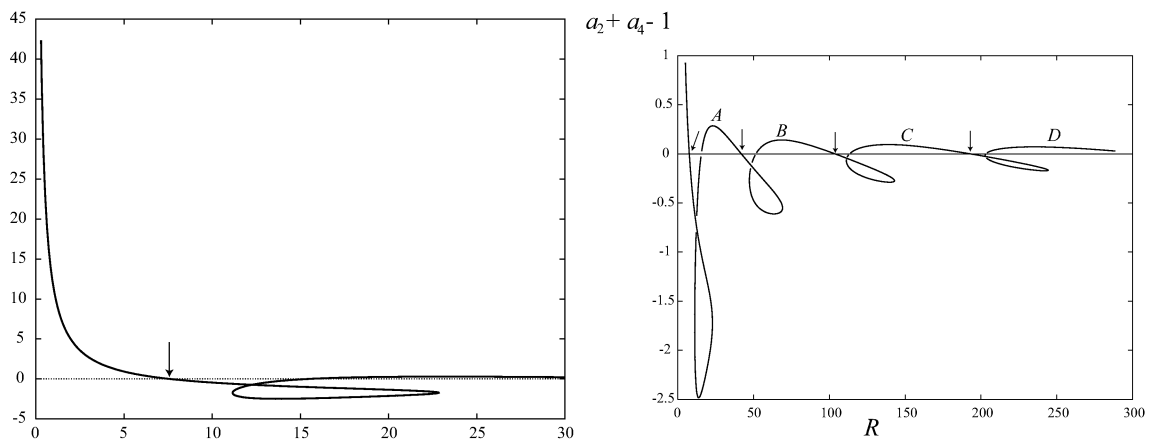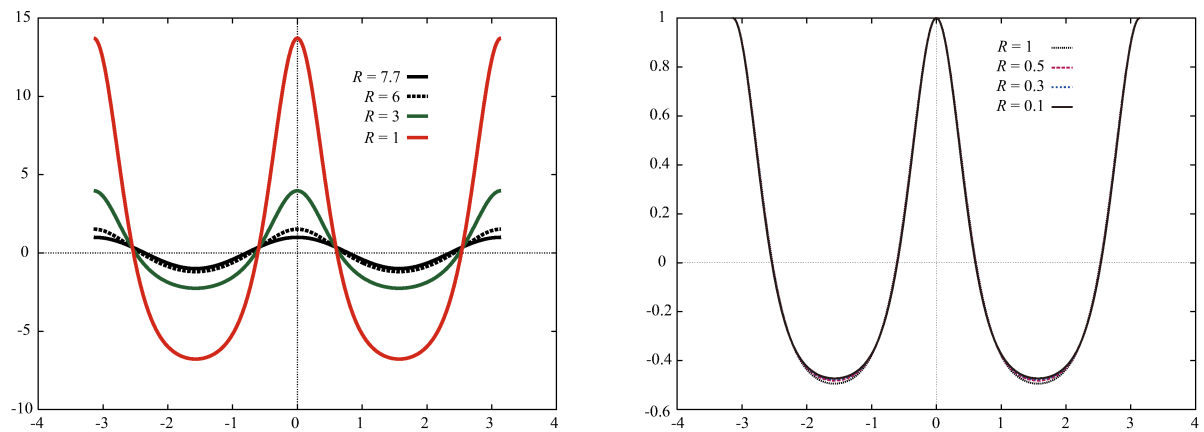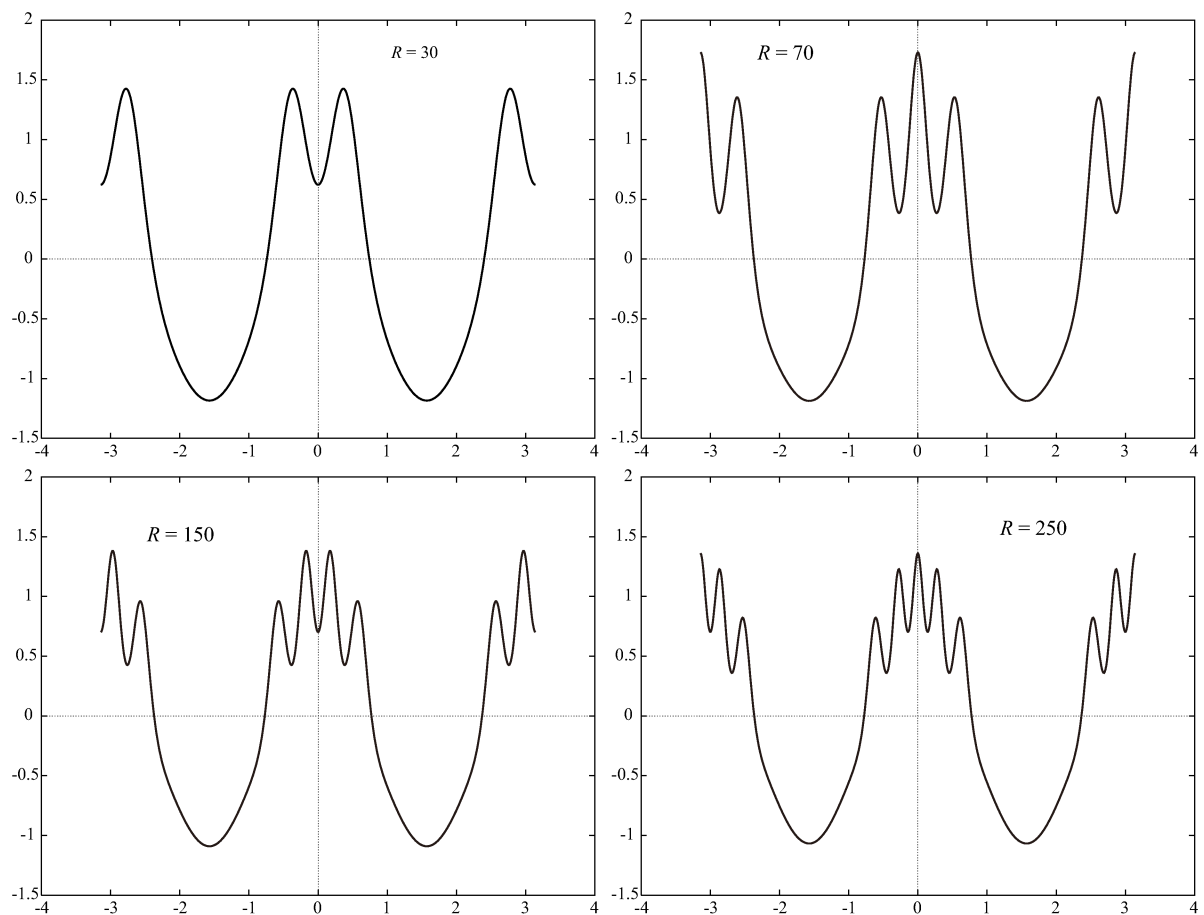

Figure 22. Diagrams. Points indicated by the arrows are bifurcation points. Other intersections are artificial, caused by the projection onto $(R, a_2 + a_4 - 1)$-plane.

Figure 23. Solutions of mode two with smaller R.

Figure 24. Solutions A, B, C, and D in Figure 22 (right).

References

[1] C. Budd, B. Dold, and A. Stuart, Blowup in a partial differential equation with conserved first integral, *SIAM J. Appl. Math.*, **53** (1993), 718–742.

[2] X.-Y. Chen and H. Matano, Convergence, asymptotic periodicity, and finite-point blow-up in one-dimensional semilinear heat equations, *J. Diff. Equations*, **78** (1989), 160–190.

[3] H. Ikeda, H. Okamoto and M. Mimura, A singular perturbation problem arising in Oseen's spiral flows, *Japan J. Indust. Appl. Math.*, **18** (2001), 393–403.

[4] H. Ikeda, K. Kondo, H. Okamoto and S. Yotsutani, On the global branches of the solutions to a nonlocal boundary-value problem arising in Oseen's spiral flows, *Commun. Pure Appl. Anal.*, **2** (2003), 373–382.

[5] S.-C. Kim and H. Okamoto, Bifurcations and inviscid limit of rhombic Navier-Stokes flows in tori, *IMA J. Appl. Math.*, **68** (2003), 119–134.

[6] S.-C. Kim and H. Okamoto, Vortices of large scale appearing in 2D stationary Navier-Stokes equations at large Reynolds numbers, *Japan J. Indus. Appl. Math.*, **27** (2010), 47–71.

[7] S.-C. Kim and H. Okamoto, The generalized Proudman-Johnson equation at large Reynolds numbers, accepted for publication in *IMA J. Appl. Math.*

[8] H. Okamoto, Localization of singularities in inviscid limit — numerical examples, in *Proceedings of Navier-Stokes equations: theory and numerical methods*, ed. R. Salvi, Longman, Pitman Research Notes in Mathematics Series vol. 388 (1998), 220–236

[9] H. Okamoto and J. Zhu, Some similarity solutions of the Navier-Stokes equations and related topics, *Taiwanese J. Math.*, **4** (2000), 65–103.

[10] F. B. Weissler, Single point blow-up for a semilinear initial value problem, *J. Diff. Equations*, **55** (1984), 204–224.